

Core Level Analysis of the Surface Charge Density Wave Transition in Sn/Ge(111)

T. E. Kidd, T. Miller, and T.-C. Chiang

*Department of Physics, University of Illinois at Urbana-Champaign, 1110 West Green Street, Urbana, Illinois 61801-3080
and Frederick Seitz Materials Research Laboratory, University of Illinois at Urbana-Champaign, 104 South Goodwin Avenue,
Urbana, Illinois 61801-2902*

(Received 9 February 1999)

Photoemission from the surface charge density wave (CDW) system Sn/Ge(111) yields a surprisingly broad Sn core level line shape at room temperature. Our study shows that it consists of three components, one associated with the normal phase and the other two associated with the CDW phase. While only the CDW phase is observed at low temperatures, both phases are present at room temperature. This is due to a 2% defect population within the Sn layer, giving rise to a remnant CDW phase above the transition temperature.

PACS numbers: 71.45.Lr, 68.35.-p, 73.20.Hb, 79.60.Dp

Recently, there has been much excitement about surface charge density wave (CDW) transitions observed in two related systems that may represent a new class of surface phenomenon [1–11]. These systems, $\frac{1}{3}$ monolayer (ML) coverages of Sn or Pb on Ge(111), were shown by scanning tunneling microscopy (STM) and electron diffraction to change from a room temperature $(\sqrt{3} \times \sqrt{3})R30^\circ$ normal phase to a low temperature (3×3) CDW phase [1–3]. The transition for Sn on Ge(111) has been studied in detail and is known to be gradual, with an apparent onset on cooling down at $T_2 = \sim 210$ K and a completion temperature of T_1 between 55 and 120 K (~ 70 K nominally) [1]. Photoemission studies of this system have yielded mixed and controversial results. A major issue is the line shape of the Sn $4d$ core level. The Sn atoms are known to occupy the T_4 adsorption site in the normal phase and should give rise to a single core level component. Yet the observed Sn core level line shape at room temperature is much too broad, suggesting a splitting into multiple components [9–13]. The origin of this splitting was unknown, and this problem had caused considerable confusion regarding the nature of the surface reconstruction and phase transition [3,5,6,9–13]. For example, a recent study by Avila *et al.* [9] showed that the line shape did not change as the sample temperature was cooled to 100 K to yield the (3×3) CDW phase. They argued that the persistent core level splitting and lack of temperature dependence could be attributed to dynamic fluctuations above the transition temperature. Contrary to previous results, our high-resolution work shows obvious temperature dependence and therefore leads to a very different conclusion. The line shape at room temperature is actually a linear superposition of three components, one from the normal phase and the other two from the CDW phase. While only the CDW phase is observed at low temperatures, both phases are present at room temperature. This is due to an inevitable, albeit small percentage (2%) of defect in the Sn layer, giving rise to a remnant CDW phase above the transition temperature T_2 .

Our photoemission measurements were carried out at the Synchrotron Radiation Center (Stoughton, Wisconsin). Spectra were taken with a hemispherical analyzer with various energy resolution settings and an acceptance cone angle of $\pm 1^\circ$, $\pm 1.5^\circ$, or $\pm 8^\circ$. The spectra shown below were all taken with a $\pm 8^\circ$ collection angle (to minimize photoelectron diffraction effects; see below) and a system resolution of about 100 meV. Further improvement in energy resolution did not result in a noticeable improvement in the appearance of the line shape. The Ge(111) substrate was prepared from a bulk crystal and oriented to within 1° . Sharp $c(2 \times 8)$ reflection high-energy electron diffraction patterns were observed for the clean (111) surface through repeated cycles of sputtering with Ar^+ ions at about 650°C followed by annealing at the same temperature. Sn was evaporated onto the Ge(111) substrate at room temperature with the amount of deposition measured by a thickness monitor. All samples were annealed to 300°C after deposition. Relative coverages, precise to within 5%, were also obtained by comparison of the ratio between the total integrated intensities of the Sn $4d$ and Ge $3d$ core levels for different coverages. As the Sn coverage was varied, different reconstructions were observed, and the observed phase boundaries were consistent with the established coverage values of low-coverage (2×2) and high-coverage $(3 \times 2\sqrt{3})$ phases of Sn/Ge(111) [13,14]. The maximum attainable Sn coverage on the surface after annealing was verified to be 1.6 ML [15].

Figure 1 shows the surface arrangement of Sn atoms in the $(\sqrt{3} \times \sqrt{3})R30^\circ$ normal phase as well as the low temperature (3×3) CDW phase at a Sn coverage of $\frac{1}{3}$ ML. STM and surface x-ray diffraction results suggest all Sn atoms occupy the T_4 site for the $(\sqrt{3} \times \sqrt{3})R30^\circ$ normal phase [3,6]. At low temperatures, a charge transfer occurs resulting in two different charge states, one positive and the other negative, relative to the initial “neutral” state. These are also referred to, in the literature, as Sn atoms with an empty dangling bond state and a filled dangling bond state, respectively. Because the positive

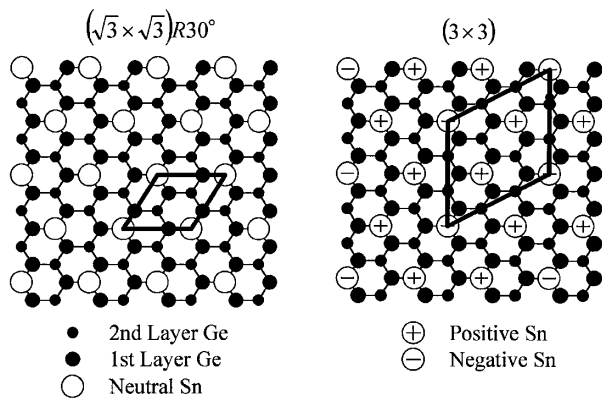


FIG. 1. Model drawings of the low temperature (3×3) and room temperature $(\sqrt{3} \times \sqrt{3})R30^\circ$ phases. A surface unit cell is outlined in each case.

and negative atoms are no longer equivalent, the unit cell size increases from $(\sqrt{3} \times \sqrt{3})R30^\circ$ to (3×3) . As shown in Fig. 1, the positive atoms are twice as many as the negative atoms; thus, the extra charge on the negative atoms is roughly twice as much as that for the positive atoms. This charge transfer is expected to cause a splitting of the Sn core level from the initial neutral position to one at a lower (higher) binding energy for the negatively (positively) charged atoms in the CDW phase.

Figure 2 displays the Sn 4d spectra taken at 300 K ($>T_2$) and 100 K ($\sim T_1$) and fitting results for a sample with a $\frac{1}{3}$ ML coverage. Contrary to previous results [9,11], our spectra are clearly temperature dependent. The

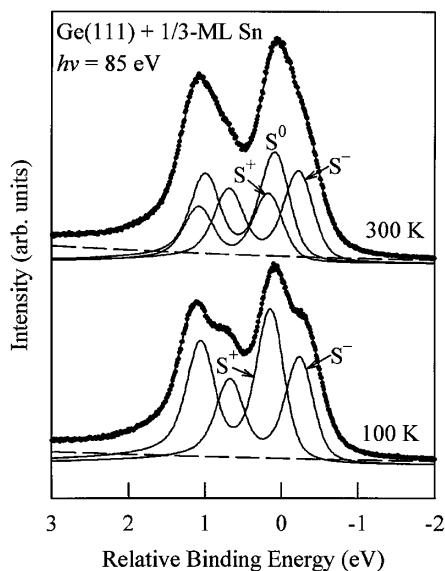


FIG. 2. Sn 4d core level spectra taken from a sample with $\frac{1}{3}$ ML Sn coverage at 300 and 100 K. The dots are data points, and the solid curves are fitting results. The dashed curves are the background functions used in the fit. Spectra were taken at normal emission with an acceptance cone of $\pm 8^\circ$.

observed line shapes were *reproducible* after multiple temperature cycles. The line shape for each spin-orbit component at 100 K suggests the presence of two components, S^- and S^+ , as indicated in Fig. 2. This is consistent with a splitting caused by the charge transfer in the CDW phase, with the S^- and S^+ components corresponding to the negative and positive Sn atoms, respectively. Changing the photon energy results in a visible modulation ($\sim 10\%$) of the relative intensities between the two components. Least-squares fitting shows that all spectra taken at 100 K can be described satisfactorily by two components, which is consistent with a pure CDW phase [1]. The 10% intensity modulation can be attributed to cross section variations and photoelectron diffraction effects. Such effects are known to be generally more important for a small analyzer acceptance cone angle. To minimize this diffraction modulation, the data shown were taken with the largest acceptance cone angle of $\pm 8^\circ$ available with our analyzer. Taking the average over a wide photon energy range (50–130 eV), the intensity ratio between S^+ and S^- is about 1.5. The expected ratio is 2 because the number of positive atoms is twice as many as the negative atoms. The 25% discrepancy is caused by defects, which will be discussed in detail below.

In comparison, the line shape at 300 K is puzzling at first sight. Ideally, all atoms are in the T_4 site, and there should be just one component. The broad line shape in Fig. 2, with a shoulder on the lower binding energy side, indicates more than one component. An attempt to fit this spectrum as well as other spectra taken at temperatures higher than 100 K with just two components was found to be unsuccessful—the peak positions shifted by up to 80 meV and the quality of the fit was poor. With the addition of a third component, the parameters for peak widths and positions all were within experimental accuracy (10 meV). Therefore, a three-component fit seems proper. The fit for the 300 K spectrum is indicated in Fig. 2 and consists of three components, S^+ and S^- as before and a new component S^0 . This new component has a binding energy in between the S^+ and S^- components and is closer to the S^+ component. It is reasonable to associate this new component with the neutral Sn atoms in the normal phase, and this assignment will be substantiated below.

As mentioned earlier, the excess charge on the negative Sn atoms is roughly twice that of the positive Sn atoms. Thus the shift of the S^- component relative to S^0 is expected to be larger than that of the S^+ component. This is consistent with our observation. As shown in Fig. 3, the relative intensities of the three core level components S^+ , S^0 , and S^- vary as the sample temperature is changed. The intensity of the S^0 component drops to zero at the lowest temperature ($\sim T_1$), where the CDW phase is fully developed. Above the transition temperature T_2 , it is a constant. This behavior is consistent with a gradual phase transition as discussed earlier.

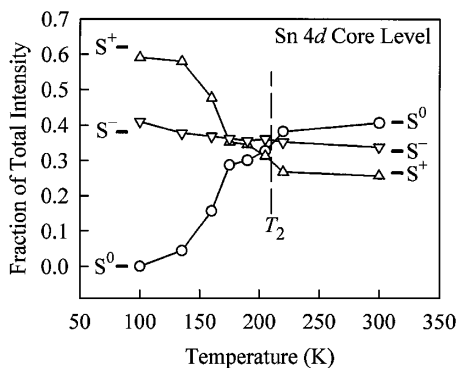


FIG. 3. Temperature dependence of the intensities of the three Sn 4d core level components S^+ , S^0 , and S^- normalized to the total intensity taken at a photon energy of 85 eV. The curves are straight line segments connecting the data points. The upper transition temperature T_2 at about 210 K is indicated by a vertical dashed line. The short horizontal line segments near the two ends of each curve indicate the expected limiting values based on our model. Spectra were taken from the same sample as in Fig. 2 and under the same conditions.

What is unusual is the persistence of the S^+ and S^- components above T_2 . However, this can be explained by the persistence of the CDW phase near defects as observed by STM [1,3]. The influence of the defect extends for about 20 Å. Figure 4 shows the typical charge state distribution near such a defect based on an analysis of STM pictures in the literature. The closest neighbors to the central defect are mostly negatively charged, while more distant neighbors can be either positively or negatively charged, forming a localized (3×3) domain. The net result is that there are more negatively charged neighbors than positively charged neighbors. Assuming a mere 2% of defect population within the Sn layer (consistent with estimates based on STM pictures in the litera-

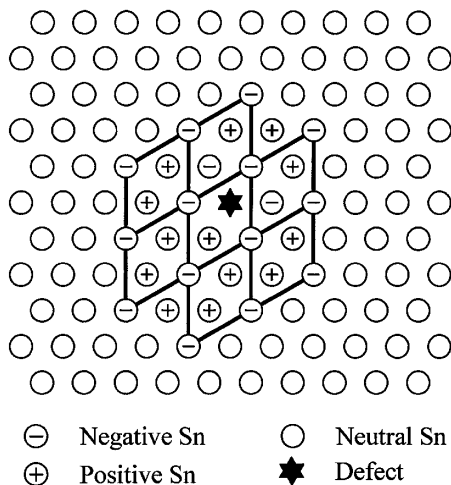


FIG. 4. Model representing CDW phase pinning about a defect at a temperature above the transition temperature T_2 .

ture), one could easily calculate the population ratios of $S^0:S^+:S^-$ to be approximately 1:0.7:0.8 at room temperature. These ratios are in agreement with the measured intensity ratios at room temperature, averaged over photon energies to minimize photoelectron diffraction effects. At low temperatures, the rest of the surface transforms into the CDW phase by growth from the pinned regions. Because of the same defect pinning, the calculated ratio between the intensities of the S^+ and S^- components is 1.5, which is less than the ideal ratio of 2 and in agreement with our observation. The horizontal bars in Fig. 3 near the two ends of each curve show the calculated relative weight for each component at both the low and high temperature limits, and there is a very good agreement with our measurements. Thus, both the room temperature and low temperature line shapes are well explained by the defect model. The reason that such a small percentage of defect can give rise to a significant contribution of S^+ and S^- in the room temperature spectra is that each defect affects a total of about 30 Sn adatom sites.

Neither STM nor photoemission can provide a definitive assignment of the defect structure, although there is some evidence for Ge substituting Sn atoms in the adlayer [3]. Figure 4 shows that each defect is surrounded by 16 negative Sn atoms and 13 positive Sn atoms. Thus, there is a net negative charge, which must be countered by a positive charge on the defect site. This is in qualitative agreement with STM measurements that the defect site itself exhibits a character of unoccupied state (positively charged).

The $(\sqrt{3} \times \sqrt{3})R30^\circ$ room temperature phase has been observed for Sn coverages up to about 0.7 ML. Further, STM work has reported nearly identical images for Sn coverages between 0.4 and 0.7 ML [13]. The implication is that the Sn atoms in excess of the ideal $\frac{1}{3}$ ML go into subsurface substitutional sites forming an alloy in the diamond lattice. Our core level studies at different Sn coverages are again consistent with these findings. As the Sn coverage is increased, the S^+ and S^0 intensities increase initially, but saturate beyond $\frac{1}{3}$ ML. In contrast, the intensity of the S^- component appears to continue to increase, suggesting that the Sn atoms alloyed into the underlying Ge lattice have nearly the same core level position as S^- . This is reasonable because the S^- adatom, with a filled dangling bond state, has an electronic structure similar to a fourfold coordinated Sn atom in the diamond lattice.

Clearly, our core level spectra presented in Fig. 2 are sharper than and qualitatively different from previous results [9,11]. For example, the overall asymmetry of our line shape at room temperature is reversed compared to that reported by Avila *et al.* [9]. This difference has led to the very different interpretation offered by that group as discussed earlier. Their publication claimed a Sn coverage of $\frac{1}{3}$ ML. However, comparison with earlier publications suggests that their coverage is likely in excess of 0.4 ML

[12,13]. As the CDW transition coverage maximum was reported to be ~ 0.43 ML [5], it is not surprising that changes in the line shape due to temperature effects could be reduced or even completely masked by the higher coverage. As mentioned above, the S^- intensity increases at coverages higher than $\frac{1}{3}$ ML. This could partly explain the different line shape observed by Avila *et al.* The angle-resolved line shape reported by Uhrberg *et al.* [11] at a coverage of 0.36 ML is again different and appears to be midway between our results and the results of Avila *et al.* Using a small acceptance cone, a coverage of 0.38 ML, and similar experimental conditions, we observed a line shape very similar to theirs. The line shape is different from the ones shown in Fig. 2 due to the coverage difference and photoelectron diffraction.

Putting all of the above together, a physically sound and consistent picture emerges. The Sn 4*d* core level line shape at low temperatures consists of two components due to charge ordering in the CDW phase. As the temperature rises above T_1 , a new component emerges at a position corresponding to the T_4 adatom in the normal phase. This evolution becomes complete at the higher transition temperature T_2 . Part of the CDW phase persists above T_2 due to static pinning of a local CDW phase by defects at the 2% level within the adatom layer.

This work was supported by the U.S. Department of Energy (Division of Materials Sciences, Office of Basic Energy Sciences) under Grant No. DEFG02-91ER45439. We acknowledge the use of the central facilities of the Frederick Seitz Materials Research Laboratory. The Synchrotron Radiation Center of the University of Wisconsin-Madison is supported by the U.S. National Science Foundation under Grant No. DMR-95-31009. An acknowledgment is made to the Donors of the Petroleum Research Fund, administered by the American Chemical Society, and to the U.S. National Science Foundation Grants No. DMR-99-75182 and No. 99-75470 for

partial personnel and equipment support in connection with the synchrotron beam line operation.

-
- [1] A. V. Melechko, J. Braun, H.H. Weitering, and E.W. Plummer, Phys. Rev. Lett. **83**, 999 (1999).
 - [2] J.M. Carpinelli, H.H. Weitering, E.W. Plummer, and R. Stumpf, Nature (London) **381**, 398 (1996).
 - [3] J.M. Carpinelli, H.H. Weitering, M. Bartkowiak, R. Stumpf, and E.W. Plummer, Phys. Rev. Lett. **79**, 2859 (1997).
 - [4] A. Goldoni, C. Cepek, and S. Modesti, Phys. Rev. B **55**, 4109 (1997).
 - [5] A. Goldoni and S. Modesti, Phys. Rev. Lett. **79**, 3266 (1997).
 - [6] A.P. Baddorf, V. Jahns, J. Zhang, J.M. Carpinelli, and E.W. Plummer, Phys. Rev. B **57**, 4579 (1998).
 - [7] A. Mascaraque, J. Avila, E.G. Michel, and M.C. Asensio, Phys. Rev. B **57**, 14758 (1998).
 - [8] J. Avila, A. Mascaraque, E.G. Michel, and M.C. Asensio, Appl. Surf. Sci. **123/124**, 626 (1998).
 - [9] J. Avila, A. Mascaraque, E.G. Michel, M.C. Asensio, G. Le Lay, J. Ortega, R. Pérez, and F. Flores, Phys. Rev. Lett. **82**, 442 (1999).
 - [10] G. Le Lay, V. Yu. Aristov, O. Boström, J.M. Layet, M.C. Asensio, J. Avila, Y. Huttel, and A. Cricenti, Appl. Surf. Sci. **123/124**, 440 (1998).
 - [11] R.I.G. Uhrberg and T. Balasubramanian, Phys. Rev. Lett. **81**, 2108 (1998).
 - [12] M. Göthelid, M. Björkqvist, T.M. Grehk, G. Le Lay, and U.O. Karlsson, Phys. Rev. B **52**, R14352 (1995).
 - [13] M. Göthelid, T.M. Grehk, M. Hammar, U.O. Karlsson, and S.A. Flodström, Surf. Sci. **328**, 80 (1995).
 - [14] S.B. DiCenzo, P.A. Bennett, D. Tribula, P. Thiry, G.K. Wertheim, and J.E. Rowe, Phys. Rev. B **31**, 2330 (1985).
 - [15] H.-J. Gossmann and L.C. Feldman, Appl. Phys. Lett. **48**, 1141 (1986).